Int. J. Electrochem. Sci., 15 **(2020)** 7337 – 7346, doi: 10.20964/2020.08.93

International Journal of
ELECTROCHEMICAL
SCIENCE
www.electrochemsci.org

Short Communication

Development of Electrochemical Immunosensor for Detecting Salbutamol by Competitive Immune Strategy

Xiao Han

Department of Physical Education, Zhengzhou University of Science and Technology, 450064, PR. China
E-mail: hanxiaope88@sina.com

Received: 30 March 2020 / *Accepted:* 2 June 2020 / *Published:* 10 July 2020

Salbutamol is a synthetic adrenergic receptor stimulant that is prohibited in competitive sports. In this work, an electrochemical sensor was fabricated using an immunoassay for the sensitive determination of the doping compound salbutamol. Polyamide amine-Au nanoparticle (PMA-Au) nanocomposites and horseradish oxidase-graphene antibodies (HRP-G-Abs) were used to amplify the signal. PMA-Au was used to immobilize the biomolecules in a stable manner, and graphene was used to increase the loaded amount of HRP. A competitive immune strategy was adopted for electrochemical sensor fabrication. The proposed immunosensor could linearly detect salbutamol from 0.1 ng/mL to 1 μg/mL, with a low detection limit of 0.03 ng/mL. In addition, the proposed immunosensor was successfully used to detect salbutamol in real samples.

Keywords: Immunosensor; Electrochemistry; Doping; Salbutamol; Graphene

1. INTRODUCTION

Salbutamol, a β-receptor agonist, is used in the treatment of asthma. If the drug is used in large doses, it will excite the central nervous system and produce protein assimilation, so it is used as a stimulant and protein assimilation agent by athletes [1–3]. There are different enforcement standards for the use of stimulants and protein assimilating agents by competitive athletes. To distinguish whether athletes used salbutamol as a stimulant or as a protein assimilating agent, the International Olympic Committee (IOC) crafted corresponding regulations [4–7]. According to the IOC, under the category of protein assimilation preparations, the definition of a positive urine test is a nonsulfate ester binding salbutamol content greater than 1000 ng.

Both salbutamol and clenbuterol can promote growth. Clenbuterol was first used as a feed additive to increase the production of livestock and poultry after robust research. In recent years, many countries have strengthened the supervision and detection of clenbuterol due to the poisoning of animal

food with clenbuterol residue [8–12]. The illegal use of clenbuterol has been greatly restricted, and criminals need to find new substitutes. Other synthetic stimulants, such as salbutamol, have similar effects. Therefore, salbutamol is also being used in animal husbandry.

Some studies have reported radioimmunoassays of salbutamol carried out by the ELISA. The detection limit of this method can reach 0.01 ng/mL. However, due to the particularity of radioimmunoassays, this technology cannot be widely used. At present, competitive ELISA is the most commonly used method to detect salbutamol, and there are commercial detection kits for sale. The kit is based on the preparation of antibodies by coupling salbutamol to BSA as an antigen and then coating onto a reaction plate. Then, the substrate is added with a color reaction and enzyme binding compound, and the absorption value is determined [13–17]. A standard curve is drawn on semilogarithmic coordinate paper, with the content of the standard product as the abscissa and the absorbance value as the ordinate [18–22]. According to the absorbance value of the sample, the sample content is determined on the standard curve, and the absorbance value is inversely proportional to the sample content. High-performance liquid chromatography (HPLC), gas chromatography-mass spectrometry (GC-MS) and capillary zone electrophoresis (CE) are the most commonly used techniques for the detection of doping residues [23–34]. HPLC has the characteristics of low detection limit, simple operation, fast results, good reproducibility and accuracy. GC-MS can be used for qualitative and quantitative analysis of a specific residue in the presence of a variety of residues. At the same time, it can effectively detect various veterinary drug residues in food, with good reproducibility, high sensitivity, speed and accuracy [35–37]. However, both of these methods have the characteristics of a tedious detection process, long detection time, expensive instruments, difficult operational procedures and high price [38–45]. CE has the advantages of high sensitivity, high resolution, high speed, low sample quantity and low cost [46,47].

In this work, an electrochemical sensor was fabricated using an immunoassay for the sensitive determination of salbutamol. Polyamide amine-Au nanoparticle (PMA-Au) nanocomposites and horseradish oxidase-graphene antibodies (HRP-G-Abs) were used to amplify the signal. PMA-Au was used to immobilize the biomolecules in a stable manner, and graphene was used to increase the loading amount of HRP. A competitive immune strategy was adopted for electrochemical sensor fabrication. In addition, the proposed immunosensor was successfully used for salbutamol detection in real samples.

2. MATERIAL AND METHODS

Salbutamol kits were purchased from the San Ying Biotechnology Co., Ltd. Poly(amino-amine), 1-(3-(dimethylamino)-propyl)-3-ethyl-carbodiimide, hydrochloride (EDC), N-hydroxysulfo-succinimide (NHS) and chloroauric acid were supplied by the Sinopharm Chemical Reagent Co., Ltd. (Shanghai, China) and used without further purification. Graphene dispersion was purchased from the Shenzhen Nano Tech Co., Ltd. All other chemicals were analytical grade. The electrochemical experiment was carried out on a CHI 760C electrochemical analyzer (Shanghai Chenhua Instrument Co., Ltd., China). A three-electrode system was adopted: a modified electrode as the working electrode, a platinum wire electrode as the counter electrode, and a saturated calomel electrode as the reference electrode (SCE). UV-vis spectra were recorded using a PerkinElmer Lambda 25 UV/Vis Spectrometer.

The solution used in the cyclic voltammetry was 0.1 M KCl containing 10 mM $K_4[Fe(CN)_6]$ and 10 mm $K_3[Fe(CN)_6]$.

The fabrication of horseradish oxidase-graphene-antibody (HRP-G-Ab) was carried out based on Malhotra et al. [48] with some modifications. Typically, 1 mL of 1 mg/mL graphene dispersion was mixed with 1 mL of mixture (including 0.4 M EDC and 0.1 M NHS) using sonication. The excessive EDC and NHS were removed using centrifugation. Then, 100 μL Ab (2.5 μg/mL) and 100 μL HRP (1 mg/mL) were added to the prepared graphene dispersion with 5 h of stirring. The excessive Ab and HRP were removed using centrifugation. Then, 1 mL of PBS (pH 7.2) was added to form HRP-G-Ab.

The preparation of PMA-Au was carried out based on Liu et al. [49] with some modifications. First, 2 mL of $HAuCl_4$ solution (0.1 mM) was mixed with 2 mL of polyamide (PAM, 0.1 mM) under stirring. Then, 2 mL of sodium citrate (0.1 mM) was slowly added for overnight reduction. The excessive sodium citrate was removed using centrifugation. The resulting material was denoted as PAM-AuNPs.

For immunosensor fabrication, the commercial Au electrode was first polished using an alumina slurry. Then, 5 μL of PAM-Au nanocomposite was drop-coated on the Au surface and dried naturally (denoted as PAM-AuNPs/Au). Then, 10 μL of salbutamol (50 ng/mL) and 10 μL of 0.5% HRP were drop-coated on the PAM-Au-modified Au surface sequentially and dried naturally (denoted as salbutamol-PAM-AuNPs/Au). Finally, 5 μL of HRP-G-Ab was drop-coated on the above modified electrode (denoted as HRP-G-Ab-salbutamol-PAM-AuNPs/Au). A schematic diagram of the modification is shown in Figure 1.

Figure 1. Schematic diagram of the fabrication of salbutamol immunosensor.

3. RESULTS AND DISCUSSION

Figure 2 shows the UV-vis spectra of PAM, $HAuCl_4$ solution and PAM-Au nanocomposite. The $HAuCl_4$ solution showed no absorption peak, while Pam showed an absorption peak at approximately 282 nm. In addition, the PAM-Au nanocomposite showed an additional peak located at approximately 601 nm, indicating the formation of Au NPs. Noble metal nanostructures have been widely used as sensing platforms to construct label-free immunosensors due to their high electrocatalytic activity and good biocompatibility [50–54]. These results suggest the successful preparation of PAM-Au nanocomposites.

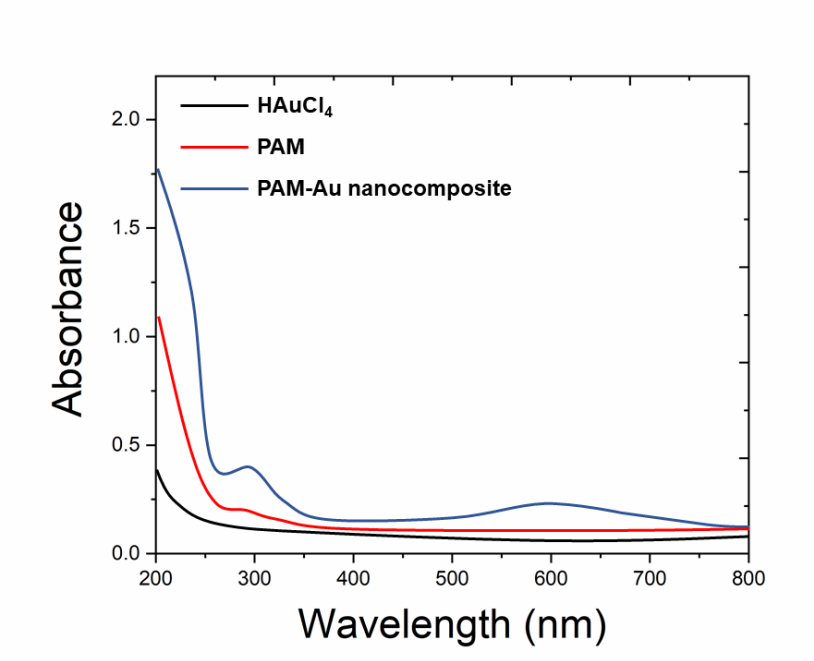

Figure 2. UV-vis spectra of PAM, $HAuCl_4$ solution and PAM-Au nanocomposite.

Then, 0.1 M KCl containing 10 mM $K_4[Fe(CN)_6]$ and 10 mm $K_3[Fe(CN)_6]$ was used as a probe to investigate the electrochemical behavior change during immunosensor fabrication. As shown in Figure 3, the bare Au electrode exhibited a well-defined oxidation and reduction of $Fe(CN)_6^{3-/4-}$. The modification of the PAM-AuNPs increased the current, suggesting that the PAM-Au nanocomposite could enhance the conductivity of the electrode. In contrast, the modification of salbutamol showed a decline in the current. In addition, the modification of HRP-G-Ab further decreased the current response, suggesting that both salbutamol and HRP-G-Ab had poor conductivity and hindered electron diffusion. These results also suggested that the proposed immunosensor fabrication process was successfully achieved. In addition, the surface of Au was more easily covered by modifying molecules, even with a smaller amount of immobilized antibody [55].

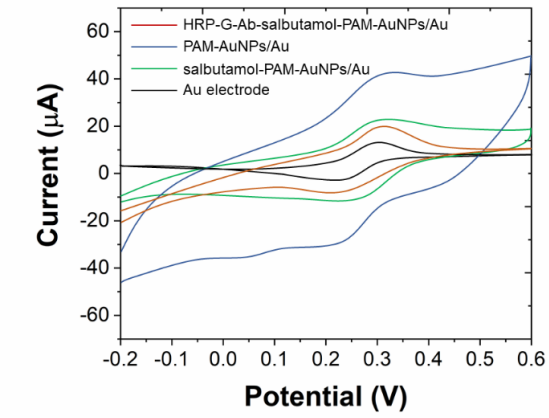

Figure 3. CV curves of bare Au electrode, PAM-AuNPs/Au, salbutamol-PAM-AuNPs/Au and HRP-G-Ab-salbutamol-PAM-AuNPs/Au at 10 mM $[Fe(CN)_6]^{4-/3-}$ solution.

The incubation time for Ab and antigen (Ag) interactions is an important parameter for immunosensors. Figure 4A shows the effect of the incubation time on the current response. The current declined significantly from 0 min to 40 min, suggesting that Ab and Ag reacted. Then, a flat platform was observed when prolonging the reaction time, suggesting that the reaction was fully achieved after 40 min, which was also observed in other studies [56,57]. Therefore, 40 min was selected for the incubation time. Figure 4B shows the effect of the H_2O_2 concentration on the immunosensor performance. The current response increased when the H_2O_2 concentration increased from 0.1 to 2 mM. No clear enhancement was observed when a higher concentration was applied. Therefore, 2 mM H_2O_2 was selected for further study.

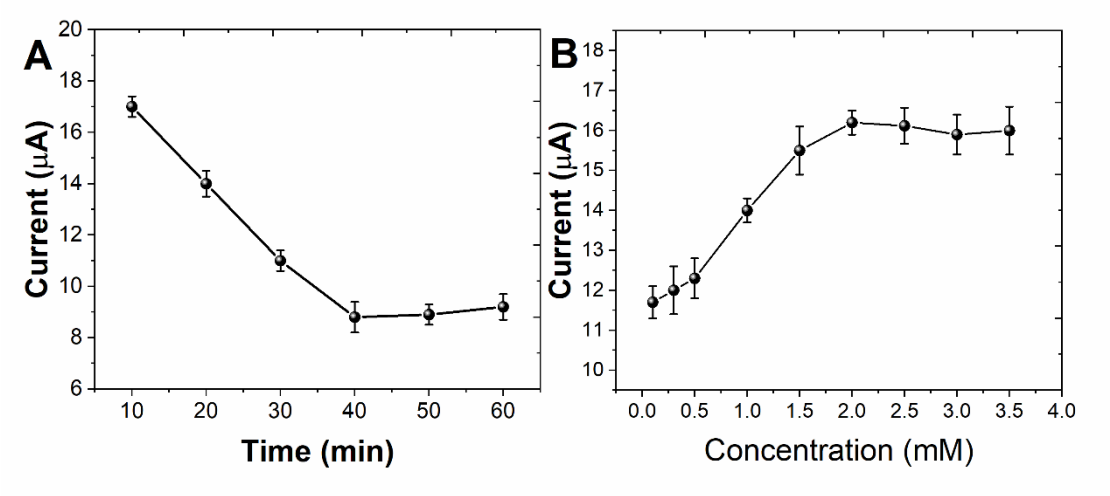

Figure 4. Effect of (A) incubation time and (B) H_2O_2 concentration on current response.

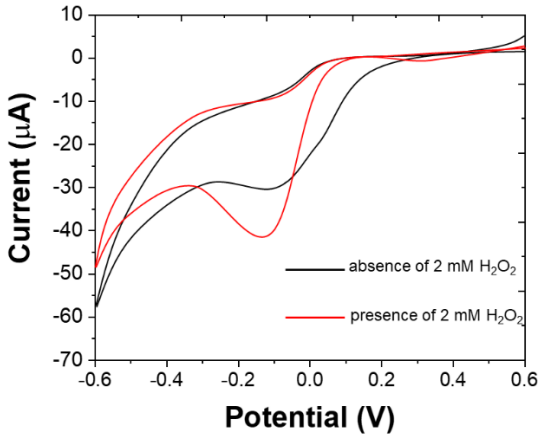

Figure 5. CV curves of the HRP-G-Ab-salbutamol-PAM-AuNPs/Au in the absence and presence of 2 mM H_2O_2.

Figure 5 shows the CV of HRP-G-Ab-salbutamol-PAM-AuNPs/Au in the absence and presence of 2 mM H_2O_2. Due to the presence of HRP, H_2O_2 could be catalyzed at a low potential. A distinct reduction process was observed in the absence of H_2O_2. The addition of H_2O_2 further increased the reduction process, suggesting that the proposed HRP-G-Ab-salbutamol-PAM-AuNPs/Au exhibited a very high sensitivity.

The proposed immunoassay is based on the competitive immune strategy. The reaction of the Ab-Ag complex is the key to the signal response. The amount of salbutamol introduced during the incubation process was directly related to the signal intensity of the proposed immunoassay during the CV scan. Ab-Ag conjugation could significantly lower the electron transfer rate and subsequently lower the signal intensity.

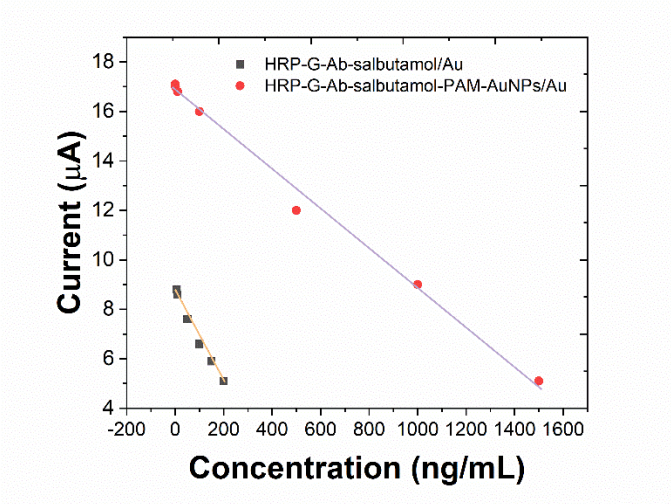

Figure 6. Calibration plots of current vs. concentration of salbutamol using HRP-G-Ab-salbutamol/Au and HRP-G-Ab-salbutamol-PAM-AuNPs/Au.

Table 1. Comparison of proposed immunosensor with previous reports.

Immunosensor	Linear range (ng/mL)	Limit of detection (ng/mL)	Reference
Capillary electrophoresis	16.46–71.7	2.39	[59]
Chemiluminescent detection	0.5-40	0.2	[60]
CS-Fe_3O_4-PAMAM-GNPs	0.11-1061	0.07	[61]
HRP-G-Ab-salbutamol-PAM-AuNPs/Au	0.1-1500	0.05	This work

As shown in Figure 6, HRP-G-Ab-salbutamol/Au could linearly detect salbutamol from 6 to 200 ng/mL with a linear equation of y(μA)=-0.01784x(ng/mL)+8.61601, while HRP-G-Ab-salbutamol-PAM-AuNPs/Au could linearly detect salbutamol from 0.1 to 1500 ng/mL with a linear equation of y(μA)=-0.00772x(ng/mL)+16.6527 and a low limit of detection of 0.02 ng/mL. Table 1 shows the

comparison of the proposed HRP-G-Ab-salbutamol-PAM-AuNPs/Au with other reports for salbutamol sensing. The proposed HRP-G-Ab-salbutamol-PAM-AuNPs/Au showed superior performance. The high sensitivity can mainly be ascribed to the following factors: (1) the large amount of immobilized Au nanoparticles can increase the loading of Ab, and (2) the good conductivity of Au nanoparticles facilitates the electron transfer of H_2O_2 at the electrode surface [58].

The reproducibility of the HRP-G-Ab-salbutamol-PAM-AuNPs/Au was investigated using five individual sensors. An RSD of 5.5% was recorded for these measurements, suggesting that the proposed HRP-G-Ab-salbutamol-PAM-AuNPs/Au exhibited excellent reproducibility. The stability of the HRP-G-Ab-salbutamol-PAM-AuNPs/Au was evaluated using one sensor for ten successive measurements. Only 7.8% of the current decrease was observed, suggesting that HRP-G-Ab-salbutamol-PAM-AuNPs/Au had good stability.

The selectivity of HRP-G-Ab-salbutamol-PAM-AuNPs/Au has been investigated using two other common dopants (clenbuterol and ractopamine). Figure 7 shows the anti-interference property of HRP-G-Ab-salbutamol-PAM-AuNPs/Au. It can be seen that 10-fold clenbuterol and ractopamine showed no clear interference during salbutamol sensing. However, the current response decreased when clenbuterol and ractopamine were above 50-fold. These results indicated that the proposed HRP-G-Ab-salbutamol-PAM-AuNPs/Au had a high specific binding affinity towards salbutamol.

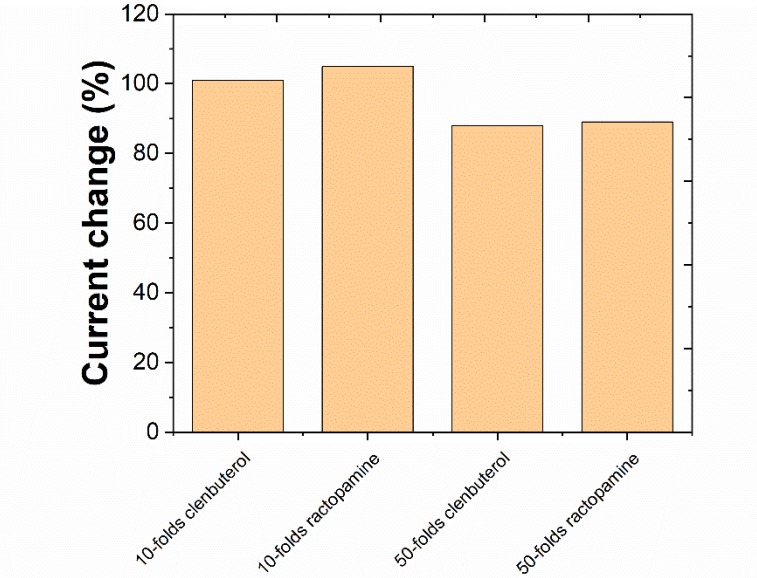

Figure 7. Anti-interference property of the HRP-G-Ab-salbutamol-PAM-AuNPs/Au.

The proposed HRP-G-Ab-salbutamol-PAM-AuNPs/Au was then used for the detection of salbutamol in real samples. A standard addition process was used. As shown in Table 2, various concentrations of salbutamol were added to a real sample. Excellent recovery performance was observed, suggesting that HRP-G-Ab-salbutamol-PAM-AuNPs/Au can be used for real sample sensing.

Table 2. Real sample test using HRP-G-Ab-salbutamol-PAM-AuNPs/Au.

Sample	Detected (ng/mL)	Added (ng/mL)	Detected (ng/mL)	Recovery (%)
1	0.00	5.00	4.98	99.60
2	0.00	10.00	10.17	101.70
3	0.00	50.00	48.95	97.90
4	0.00	100.00	101.54	101.54

4. CONCLUSION

In this work, an electrochemical sensor was fabricated using an immunoassay for the sensitive determination of salbutamol. Polyamide amine-Au nanoparticle (PMA-Au) nanocomposites and horseradish oxidase-graphene antibodies (HRP-G-Abs) were used to amplify the signal. PMA-Au was used to immobilize the biomolecules in a stable manner, and graphene was used to increase the loaded amount of HRP. A competitive immune strategy was adopted for electrochemical sensor fabrication. In addition, the proposed immunosensor was successfully used to detect salbutamol in real samples.

References

1. J. Pleadin, A. Vulić, R. Stojković, N. Peršil, M. Mitak, M. Zadravec, *Rev. Anal. Chem.*, 29 (2010) 39–50.
2. C. Xie, F. Chen, T. Yang, *Anal. Biochem.*, 426 (2012) 118–125.
3. P. Raksawong, K. Chullasat, P. Nurerk, P. Kanatharana, F. Davis, O. Bunkoed, *Anal. Bioanal. Chem.*, 409 (2017) 4697–4707.
4. Z. Yan, T. Hu, W. Guo, A. Deng, J. Di, *Bioprocess Biosyst. Eng.*, 37 (2014) 651–657.
5. Y. Chen, M. Xie, *RSC Adv.*, 5 (2015) 95401–95404.
6. X. Yang, F. Wu, D.-Z. Chen, H.-W. Lin, *Sens. Actuators B Chem.*, 192 (2014) 529–535.
7. Z. Cui, Y. Cai, D. Wu, H. Yu, Y. Li, K. Mao, H. Wang, H. Fan, Q. Wei, B. Du, *Electrochimica Acta*, 69 (2012) 79–85.
8. J. Zhang, F. Cai, A. Deng, J. Li, *Electroanalysis*, 26 (2014) 873–881.
9. J. Tang, Z. Liu, J. Kang, Y. Zhang, *Anal. Bioanal. Chem.*, 397 (2010) 3015–3022.
10. Y. Wu, F. Xu, H. Jiang, X. Tao, K. Zhu, W. Liu, Y. Cui, X. Huang, S. Ding, *Anal. Lett.*, 47 (2014) 2761–2773.
11. C. Li, J. Li, W. Jiang, S. Zhang, J. Shen, K. Wen, Z. Wang, *J. Agric. Food Chem.*, 63 (2015) 10556–10561.
12. Y. Lei, X. Li, M.S.H. Akash, L. Zhou, X. Tang, W. Shi, Z. Liu, S. Chen, *J. Pharm. Biomed. Anal.*, 107 (2015) 204–208.
13. F. Tahernejad-Javazmi, M. Shabani-Nooshabadi, H. Karimi-Maleh, *Compos. Part B Eng.*, 172 (2019) 666–670.
14. A.F. Mulaba-Bafubiandi, H. Karimi-Maleh, F. Karimi, M. Rezapour, *J. Mol. Liq.*, 285 (2019) 430–435.
15. S. Jahandari, M.A. Taher, H. Karimi-Maleh, A. Khodadadi, E. Faghih-Mirzaei, *J. Electroanal. Chem.*, 840 (2019) 313–318.
16. H. Karimi-Maleh, F. Karimi, M. Rezapour, M. Bijad, M. Farsi, A. Beheshti, S.-A. Shahidi, *Curr. Anal. Chem.*, 15 (2019) 410–422.
17. F. Hosseini, M. Ebrahimi, H. Karimi-Maleh, *Curr. Anal. Chem.*, 15 (2019) 177–182.
18. G. Zhu, Y. Hu, J. Gao, L. Zhong, *Anal. Chim. Acta*, 697 (2011) 61–66.

19. E. Zvereva, A. Zherdev, C. Xu, B. Dzantiev, *Food Control*, 86 (2018) 50–58.
20. H. Gao, J. Han, S. Yang, Z. Wang, L. Wang, Z. Fu, *Anal. Chim. Acta*, 839 (2014) 91–96.
21. L. Hu, P. Zuo, B.-C. Ye, *Anal. Biochem.*, 405 (2010) 89–95.
22. K. Yan, H. Zhang, W. Hui, H. Zhu, X. Li, F. Zhong, C. Chen, *J. Food Drug Anal.*, 24 (2016) 277–283.
23. K.-C. Lin, C.-P. Hong, S.-M. Chen, *Sens. Actuators B Chem.*, 177 (2013) 428–436.
24. L. Liu, H. Kuang, C. Peng, L. Wang, C. Xu, *Anal. Methods*, 6 (2014) 4228–4233.
25. G. Chen, X. Huang, S. Li, X. Kong, B. Huai, *Food Agric. Immunol.*, 25 (2014) 322–331.
26. X. Zhang, Y. Chu, H. Yang, K. Zhao, J. Li, H. Du, P. She, A. Deng, *Food Anal. Methods*, 9 (2016) 3396–3406.
27. L. Fu, Y.-H. Zheng, Z.-X. Fu, *Chem. Pap.*, 69 (2015) 655–661.
28. L. Fu, T. Tamanna, W.-J. Hu, A. Yu, *Chem. Pap.*, 68 (2014) 1283–1297.
29. A. Wang, L. Fu, T. Rao, W. Cai, M.-F. Yuen, J. Zhong, *Opt. Mater.*, 42 (2015) 548–552.
30. L. Fu, Y. Zheng, P. Zhang, H. Zhang, W. Zhuang, H. Zhang, A. Wang, W. Su, J. Yu, C.-T. Lin, *Biosens. Bioelectron.*, 120 (2018) 102–107.
31. A. Wang, H.P. Ng, Y. Xu, Y. Li, Y. Zheng, J. Yu, F. Han, F. Peng, L. Fu, *J. Nanomater.*, 2014 (2014).
32. L. Fu, G. Chen, N. Jiang, J. Yu, C.-T. Lin, A. Yu, *J. Mater. Chem. A*, 4 (2016) 19107–19115.
33. L. Fu, G. Lai, H. Zhang, A. Yu, *J. Nanosci. Nanotechnol.*, 15 (2015) 4325–4331.
34. L. Fu, Y. Zheng, A. Wang, *Int J Electrochem Sci*, 10 (2015) 3518–3529.
35. X. Lu, H. Zheng, X.-Q. Li, X.-X. Yuan, H. Li, L.-G. Deng, H. Zhang, W.-Z. Wang, G.-S. Yang, M. Meng, *Food Chem.*, 130 (2012) 1061–1065.
36. M. Liu, B. Ning, L. Qu, Y. Peng, J. Dong, N. Gao, L. Liu, Z. Gao, *Sens. Actuators B Chem.*, 161 (2012) 124–130.
37. H. He, T. Sun, W. Liu, Z. Xu, Z. Han, L. Zhao, X. Wu, B. Ning, J. Bai, *Microchem. J.* (2020) 104804.
38. L. Fu, A. Wang, K. Xie, J. Zhu, F. Chen, H. Wang, H. Zhang, W. Su, Z. Wang, C. Zhou, S. Ruan, *Sens. Actuators B Chem.*, 304 (2020) 127390.
39. L. Fu, K. Xie, D. Wu, A. Wang, H. Zhang, Z. Ji, *Mater. Chem. Phys.*, 242 (2020) 122462.
40. N. Sabet Sarvestani, M. Tabasizadeh, M. Hossein Abbaspour-Fard, H. Nayebzadeh, H. Karimi-Maleh, T. Chu Van, M. Jafari, Z. Ristovski, R.J. Brown, *Fuel*, 272 (2020) 117728.
41. Y. Xu, Y. Lu, P. Zhang, Y. Wang, Y. Zheng, L. Fu, H. Zhang, C.-T. Lin, A. Yu, *Bioelectrochemistry*, 133 (2020) 107455.
42. H. Karimi-Maleh, K. Cellat, K. Arıkan, A. Savk, F. Karimi, F. Şen, *Mater. Chem. Phys.*, 250 (2020) 123042.
43. M. Zhang, B. Pan, Y. Wang, X. Du, L. Fu, Y. Zheng, F. Chen, W. Wu, Q. Zhou, S. Ding, S. Zhao, *ChemistrySelect*, 5 (2020) 5035–5040.
44. H. Jia, P. Gao, H. Ma, D. Wu, B. Du, Q. Wei, *Bioelectrochemistry*, 101 (2015) 22–27.
45. H. Karimi-Maleh, O.A. Arotiba, *J. Colloid Interface Sci.*, 560 (2020) 208–212.
46. Y. Lei, X. Yao, D. Zhang, L. Zhou, W. Lu, S. Chen, *Anal. Methods*, 7 (2015) 5635–5640.
47. T. Dong, L. Hu, K. Zhao, A. Deng, J. Li, *Anal. Chim. Acta*, 945 (2016) 85–94.
48. K. Esumi, K. Miyamoto, T. Yoshimura, *J. Colloid Interface Sci.*, 254 (2002) 402–405.
49. S. Liu, Q. Lin, X. Zhang, X. He, X. Xing, W. Lian, J. Huang, *Sens. Actuators B Chem.*, 156 (2011) 71–78.
50. H. Karimi-Maleh, F. Karimi, S. Malekmohammadi, N. Zakariae, R. Esmaeili, S. Rostamnia, M.L. Yola, N. Atar, S. Movaghgharnezhad, S. Rajendran, A. Razmjou, Y. Orooji, S. Agarwal, V.K. Gupta, *J. Mol. Liq.*, 310 (2020) 113185.
51. T. Zabihpour, S.-A. Shahidi, H. Karimi-Maleh, A. Ghorbani-HasanSaraei, *Microchem. J.*, 154 (2020) 104572.

52. L. Fu, Y. Zheng, P. Zhang, H. Zhang, Y. Xu, J. Zhou, H. Zhang, H. Karimi-Maleh, G. Lai, S. Zhao, W. Su, J. Yu, C.-T. Lin, *Biosens. Bioelectron.*, 159 (2020) 112212.
53. J. Mohanraj, D. Durgalakshmi, R.A. Rakkesh, S. Balakumar, S. Rajendran, H. Karimi-Maleh, *J. Colloid Interface Sci.*, 566 (2020) 463–472.
54. H. Alamgholiloo, S. Rostamnia, A. Hassankhani, X. Liu, A. Eftekhari, A. Hasanzadeh, K. Zhang, H. Karimi-Maleh, S. Khaksar, R.S. Varma, M. Shokouhimehr, *J. Colloid Interface Sci.*, 567 (2020) 126–135.
55. C.-H. Lin, C.-C. Wu, Y.-F. Kuo, *J. Electroanal. Chem.*, 768 (2016) 27–33.
56. L. Shen, P. He, *Electrochem. Commun.*, 9 (2007) 657–662.
57. Y. Wu, P. Dong, A. Deng, J. Di, *Anal. Methods*, 5 (2013) 5222–5226.
58. Z. Cui, Y. Cai, D. Wu, H. Yu, Y. Li, K. Mao, H. Wang, H. Fan, Q. Wei, B. Du, *Electrochimica Acta*, 69 (2012) 79–85.
59. J. Ouyang, J.L. Duan, W.R. Baeyens, J.R. Delanghe, *Talanta*, 65 (2005) 1–6.
60. H. Gao, J. Han, S. Yang, Z. Wang, L. Wang, Z. Fu, *Anal. Chim. Acta*, 839 (2014) 91–96.
61. S. Liu, Q. Lin, X. Zhang, X. He, X. Xing, W. Lian, J. Huang, *Sens. Actuators B Chem.*, 156 (2011) 71–78.